Applied Catalysis B: Environmental 84 (2008) 715–722

Contents lists available at ScienceDirect

Applied Catalysis B: Environmental

journal homepage: www.elsevier.com/locate/apcatb

In situ DRIFTS study of the effect of structure (CeO_2–La_2O_3) and surface (Na) modifiers on the catalytic and surface behaviour of Pt/γ-Al_2O_3 catalyst under simulated exhaust conditions

V. Matsouka [a], M. Konsolakis [a], R.M. Lambert [b], I.V. Yentekakis [a,*]

[a] Laboratory of Physical Chemistry and Chemical Processes, Department of Sciences, Technical University of Crete, 73100 Chania, Crete, Greece
[b] Department of Chemistry, University of Cambridge, UK

ARTICLE INFO

Article history:
Received 21 March 2008
Received in revised form 23 May 2008
Accepted 3 June 2008
Available online 12 June 2008

Keywords:
Platinum
Sodium
Promotion
CeO_2
La_2O_3
Simulated exhaust conditions
Isocyanates
DRIFT

ABSTRACT

The nature and relative populations of adsorbed species formed on the surface of un-promoted and sodium-promoted Pt catalysts supported either on bare Al_2O_3 or CeO_2/La_2O_3-modified Al_2O_3, were investigated by in situ diffuse reflectance infrared Fourier transform spectroscopy (DRIFTS) under simulated automobile exhaust conditions (CO + NO + C_3H_6 + O_2) at the stoichiometric point. The DRIFT spectra indicate that interaction of the reaction mixture with the Pt/Al_2O_3 catalyst leads mainly to formation of formates and acetates on the support and carbonyl species on partially positively charged Pt atoms ($Pt^{\delta+}$). Although enrichment of Al_2O_3 with lanthanide elements (CeO_2 and La_2O_3) does not significantly modify the carboxylate species formed on the support, it causes significant modification of the oxidation state of Pt, as indicated by the appearance of a substantial population of carbonyl species on reduced Pt sites (Pt^0–CO). This modification of the Pt component is enhanced when Na-promotion is used, leading to formation of carbonyl species only on electron enriched Pt (i.e., fully reduced Pt^0 sites) and to the formation of NCO on these Pt entities (2180 cm^{-1}). The latter are thought to result from enhanced NO dissociation at Na-modified Pt sites. These results correlate well with observed differences in the catalytic performance of the three different systems.

1. Introduction

Three-way automotive catalytic converters (TWCs) employ a well established technology for abatement of NOx, CO and hydrocarbon emissions, based variously on the catalytic properties of Pt, Pd and Rh: the latter is especially effective for NO dissociation and is therefore the key component responsible for NOx reduction [1–4]. However, TWC systems require use of (scarce) Rh, emit low but significant N_2O emission and are not well suited to recycling because they contain more than one noble metal. Accordingly, considerable effort has focused on enhancing the de-NOx catalytic performance of monometallic Pt and Pd systems. We have recently shown that significant improvements can be achieved by use of electropositive promoters (alkalis or alkaline earths) which strongly enhance activity and selectivity in regard to CO [5] and hydrocarbon oxidation [6,7]; NOx reduction by CO [8–10] or hydrocarbons [9–16] both in the absence [12–16] and presence of oxygen [9–11]. Other workers have made similar progress [e.g. 17–20]. Potential practical significance is the development of novel formulations for catalytic converters in which only one Pt group metal need be used, yielding the advantages mentioned above.

A theoretical explanation [21] of the electronic mode of action of electropositive promoters in these catalytic systems is available [5–16] which consistently accounts for all the experimental observations. Such promoters induce strengthening of the chemisorptive bonds of electron-accepting adsorbates (e.g., CO, NO, O_2 and their dissociation products) promoting their adsorption; correspondingly the chemisorptive bonds of electron donating adsorbates are weakened (e.g., hydrocarbons and their dissociative chemisorption fragments) inhibiting their adsorption. Thus in the case of NO adsorption, alkali-induced enhancement of the metal–NO chemisorption bond is accompanied by weakening of the N–O bond, favouring dissociative chemisorption, thus enhancing the rate of NO reduction. In this connection, we have recently reported in situ DRIFTS studies [22] of the interaction of NO with Na-modified Pt(Na)/γ-Al_2O_3 catalysts: Na promotion resulted in pronounced and progressive red shifts of the N–O

* Corresponding author. Tel.: +30 28210 37752; fax: +30 28210 37844.
E-mail address: yyentek@science.tuc.gr (I.V. Yentekakis).

0926-3373/$ – see front matter © 2008 Elsevier B.V. All rights reserved.
doi:10.1016/j.apcatb.2008.06.004

stretching frequency associated with molecular NO adsorbed on the Pt component of the catalyst.

In the present paper we expand our in situ DRIFTS studies to more complex and interesting systems investigated under realistic conditions—simulated automotive exhaust at the stoichiometric point, i.e. TWC conditions. The effects of support-mediated promotion (modification of Al_2O_3 with CeO_2 and La_2O_3) and of promotion of the Pt component by Na were investigated. Direct spectroscopic evidences are pursued for the way of action of these support-mediated and surface-induced promotional phenomena on the TWC catalytic chemistry, where a large number of reactants and reaction intermediates are simultaneously compete and interact on catalytic active sites.

2. Experimental methods

2.1. Materials

Table 1 summarizes the composition of the samples studied. These include Pt-free reference materials, a reference Pt/γ-Al_2O_3 (designated Pt/Al), a Pt/γ-Al_2O_3–(CeO_2–La_2O_3) catalyst (designated Pt/Al–(Ce–La)), a sodium-promoted Pt(Na)/γ-Al_2O_3 catalyst (designated Pt(Na)/Al), and a doubly-promoted Pt(Na)/γ-Al_2O_3–(CeO_2–La_2O_3) catalyst (designated Pt(Na)/Al–(Ce–La)). These materials were prepared as follows: bare γ-Al_2O_3 (Aldrich, 155 m^2/g) or 6 wt.% CeO_2 and 2 wt.% La_2O_3 enriched γ-Al_2O_3 supports, were impregnated in aqueous solution of dinitrodiamine-Pt and $NaNO_3$ containing appropriate Pt and Na concentrations so as to yield 0.5 wt.% Pt and 10 wt.% Na loadings (in the latter cases, the support material was prepared by intermixing rare oxides powders, particle size <5 μm, with the alumina). The resulting suspensions were dried at 110 °C overnight and then calcined at 600 °C for 2 h.

Catalytic performance was evaluated under simulated exhaust conditions at the stoichiometric point (0.1% NO + 0.1067% C_3H_6 + 0.7% CO + 0.78% O_2, balance He at 1 bar) and a total GHSV of 50,500 h^{-1} (corresponding to an overall flow rate of 200 L/h) in a tubular quartz continuous flow reactor (24 mm i.d.), after deposition of the catalytic material as a washcoat on cylindrical cordierite honeycomb monoliths (400 cells/in.^{2} and ~4 cm^3 volume). After washcoat deposition, the following procedure was repeated until the washcoat amounted to 20 ± 0.5 wt.% of the total monolith weight, namely 2 ± 0.1 g: immersion of the monoliths in the appropriate stirred slurry of the catalytic material followed by drying at 110 °C for 2 h and then at 600 °C for 2 h. Product analysis was by means of on-line gas chromatography (Shimatzu-14B) for CO, CO_2, O_2, C_3H_6, N_2 and N_2O and continuous on-line chemiluminescence NOx-analysis (Thermo Environmental Instruments 42C) for NO and NO_2. In order to ensure stability, the monoliths were run under reaction conditions for 24 h at 700 °C and then at 550 °C for 5 days before acquisition of catalytic performance data.

Table 1
Coding and constitution of catalysts studied

Catalyst code	Catalysts constitution (wt.%)				
	Pt	Na	Al_2O_3	CeO_2	La_2O_3
Al	–	–	100	–	–
Al–(Ce–La)	–	–	92	6	2
Na/Al	–	10	90	–	–
Na/Al–(Ce–La)	–	10	82	6	2
Pt/Al	0.5	–	99.5	–	–
Pt/Al–(Ce–La)	0.5	–	91.5	6	2
Pt(Na)/Al	0.5	10	89.5	–	–
Pt(Na)/Al–(Ce–La)	0.5	10	81.5	6	2

2.2. In situ DRIFTS studies

Diffuse reflectance IR spectra were collected using an Excalibur FTS 3000 spectrometer, equipped with an MCT detector cooled by liquid nitrogen in conjunction with a Specac Environmental Chamber DRIFT cell that allowed in situ sample treatment. Spectra were obtained with resolution of 2 cm^{-1} with accumulation of 64 scans. During these measurements the external optics were purged with CO_2-free dry air generated from an air purifier system (Claind Italy, CO_2-PUR model). Catalyst samples (~80 mg) in powder form were carefully flattened in order to maximize the intensity of the reflected IR beam.

The sample chamber was supplied at 1 bar pressure by the appropriate gas mixtures delivered *via* a gas-mixing unit. Mixture composition was controlled by mass flow controllers (MKS type 247) connected to compressed gas cylinders containing 7.83% NO in He; 10% C_3H_6 in He, 10% CO in He; 20.7% O_2 in He; 100% H_2 and ultrapure He (Air Liquide certified gases). The total flow rate was maintained at 80 cm^3/min and before to each experiment the catalyst was pre-treated as follows:

(i) Oxidation at 400 °C with 20.7% O_2/He flow for 30 min.
(ii) Purging with He flow at 400 °C for 30 min.
(iii) Reduction at 400 °C with 20% H_2/He flow for 1 h.
(iv) Purging with He flow at 400 °C for 30 min.
(v) Background spectra acquisition under He flow at the desired temperatures.

Two types of DRIFT experiments were performed:

(i) Steady-state experiments at constant feed composition corresponding to simulated automotive exhaust conditions at the stoichiometric point (0.1% NO + 0.1067% C_3H_6 + 0.7% CO + 0.78% O_2). The system was allowed to stabilize for 30 min in order to attain steady-state band intensities, spectra being recorded as a function of temperature at the interval of 200–450 °C.
(ii) Transient experiments involving (a) exposure of the catalysts to a flux of 0.1% NO + 0.78% O_2 for 1 h at 200 °C followed by (b) a mixture of 0.1067% C_3H_6 + 0.7% CO. Change in band intensities as a function of time and temperature (200–450 °C) were recorded.

3. Results and discussion

3.1. Catalytic performance of Pt/Al, Pt(Na)/Al, Pt/Al–(Ce–La) and Pt(Na)/Al–(Ce–La) under simulated automotive exhaust conditions

Fig. 1 shows the steady state performance of the catalysts at a constant temperature of 350 °C under simulated exhaust conditions with respect to CO, C_3H_6 and NO conversion; selectivity towards to N_2 is also shown. Table 2 summarizes catalyst performance in terms of T_0 (ignition temperature), T_{50} (temperature for 50% conversion, i.e., *light-off* temperature) and T_{100} (temperature for 100% conversion) for C_3H_6, CO and NO. The corresponding N_2 selectivities are also given. It is clear from these results that both support-mediated promotion alone (by ceria-lanthana) and sodium promotion alone significantly improve all aspects of performance, and to a similar degree, relative to the unpromoted system. Interestingly, the best performance of all is shown by the doubly-promoted catalyst Pt(Na)/Al–Ce–La.

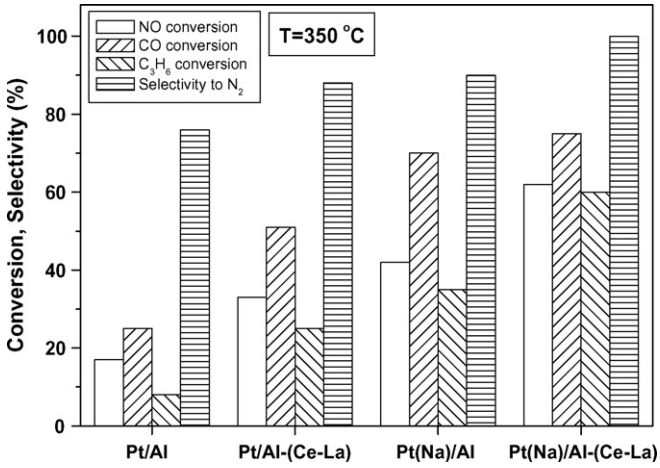

Fig. 1. Conversion and selectivity performance of indicated catalysts under simulated exhaust conditions at the stoichiometric point at 350 °C. *Reaction conditions*: 0.1% NO + 0.1067% C_3H_6 + 0.7% CO + 0.78% O_2, balance He at 1 bar and a total GHSV = 50,500 h^{-1}.

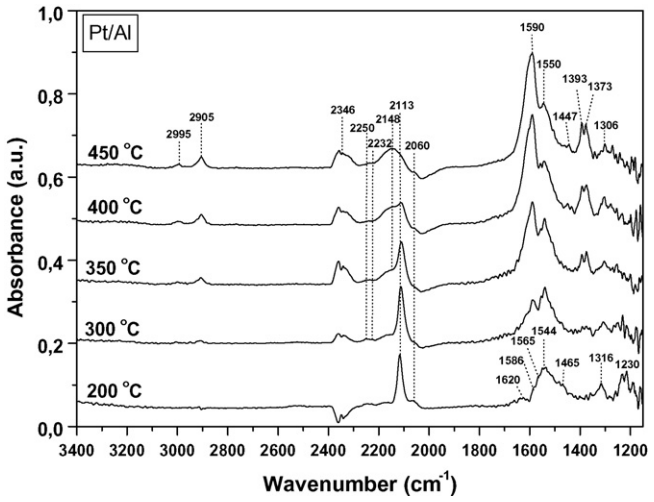

Fig. 2. DRIFT spectra of Pt/Al catalyst at various temperatures under simulated exhaust conditions. FT-IR chamber feed: 0.1% NO + 0.1067% C_3H_6 + 0.7% CO + 0.78% O_2; total flow 80 cm^3/min. Each spectrum has been taken 30 min after the desired temperature reached.

3.2. Steady-state in situ DRIFTS experiments under simulated automotive exhaust conditions

Fig. 2 depicts IR spectra of adsorbed species present on the surface of the unpromoted Pt/Al_2O_3 catalyst under simulated automotive exhaust conditions at temperatures in the interval of 200–450 °C. Two prominent groups of bands were apparent over the whole temperature range: one at 1650–1100 cm^{-1} and another at the 2300–1800 cm^{-1}. The former may be attributed to carbonate, carboxylate and nitroxy species on the Al_2O_3 support. The 2300–1800 cm^{-1} region is most likely associated with adsorbed species on Pt sites and/or with adsorbed species the formation of which require the existence of both active metal and the supporting material (i.e., initially formed on the metal sites and then migrated to the support). These assignments are validated by comparison with analogous data obtained with bare Al_2O_3 (Fig. 3).

The principal bands observed and the corresponding assignments are summarized in Table 3. In particular, with Pt/Al_2O_3 at 200 °C (Fig. 2) two strong bands are observed at 2300–1800 cm^{-1}. The weak band at 2060 cm^{-1} is characteristic of linearly adsorbed CO on reduced Pt sites, whereas the high intensity band at 2113 cm^{-1} is attributed to CO adsorbed on partially positively charged Pt sites ($Pt^{\delta+}$) [23–28]. This indicates that under the prevailing conditions the Pt component is mainly in its oxidized form. Similar bands at 2121 and 2067 cm^{-1} observed by Alexeev et al. [27] in a DRIFT study of the CO + O_2 coadsorption over Pt/Al_2O_3 were correspondingly assigned. At elevated temperatures (>∼200 °C), they found that only the band at 2121 cm^{-1} survived, which they therefore ascribed to relatively unreactive CO species adsorbed at $Pt^{\delta+}$ sites [27].

Assignment of the low frequency bands is more complicated as a number species (carboxylates, carbonates, and nitroxy) with

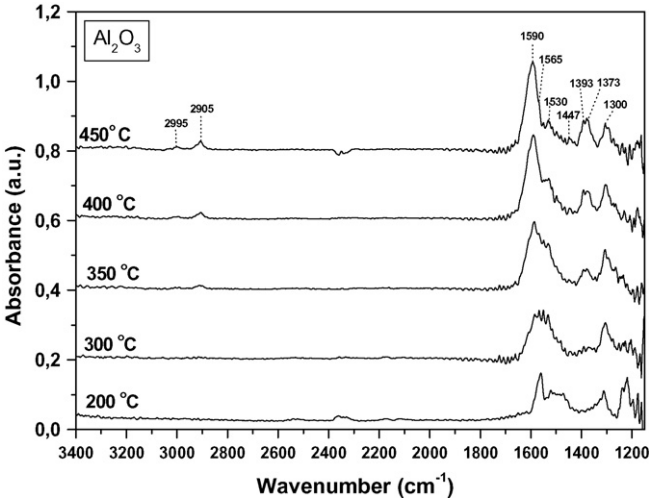

Fig. 3. DRIFT spectra of bare Al_2O_3 at various temperatures under simulated exhaust conditions. FT-IR chamber feed: 0.1% NO + 0.1067% C_3H_6 + 0.7% CO + 0.78% O_2; total flow 80 cm^3/min. Each spectrum has been taken 30 min after the desired temperature reached.

overlapping spectra could be present under the prevailing conditions. However, literature data and additional results we obtained for NO + O_2, CO + O_2 or C_3H_6 + O_2 adsorption on alumina based samples (not shown here) indicates the following assignments: bands at 1620, 1586, 1565 and 1544 cm^{-1} observed at 200 °C (Fig. 2) are due to nitrates (bridging, bidentate, and monodentate) adsorbed on Al_2O_3; that at 1465 cm^{-1} is attributed to ν(N═O) of a linear nitrite while the bands at 1230 and 1316 are

Table 2
Catalysts' performance in terms of T_0 (ignition temperature), T_{50} (temperature for 50% conversion, i.e., *light-off* temperature) and T_{100} (temperature for 100% conversion) for C_3H_6, CO and NO conversions under simulated exhaust conditions

Catalyst code	C_3H_6 conversion			CO conversion			NO conversion/N_2 selectivity		
	T_0	T_{50}	T_{100}	T_0	T_{50}	T_{100}	T_0	T_{50}	T_{100}
Pt/Al	345	400	–	315	380	–	335/74	400/94	–
Pt/Al–(Ce–La)	300	370	485	300	350	400	320/71	370/92	415/99
Pt(Na)/Al	275	360	430	260	330	400	305/70	360/84	405/97
Pt(Na)/Al–(Ce–La)	245	340	435	270	330	375	280/100	340/100	395/100

Table 3
Bands position and the corresponding assignments of surface species in DRIFT spectra

Surface species	Peak position (cm^{-1})	Infrared vibration	Reference
Chelating nitro or bridging nitrite	1316	$\nu_{as}(NO_2)$	22 and references therein
	1230	$\nu_s(NO_2)$	
Nitrite ion (NO_2^-)	1260	$\nu_{as}(NO_2)$	
Linear nitrite	1465	$\nu(N{=}O)$	
Nitrates	1620–1530	$\nu(N{=}O)$ or $\nu_{as}(NO_2)$	
Formates	1373	$\nu_s(COO^-)$	[23,24,32–36]
	1393	$\delta(CH)$	
	1590	$\nu_{as}(COO^-)$	
Adsorbed hydrocarbon fragments	2905	–CH stretching	[23,24,33]
	2995		
Acetates	1447	$\nu_s(COO^-)$	[23,24,32–36]
	1550	$\nu_{as}(COO^-)$	
Carbonates	1600 and 1334	$\nu(CO_3)$	[43–45]
Carbonyls (>C═O) on reduced Pt	2050–2080	$\nu(CO)$	[23–28]
Carbonyls (>C═O) on partially oxidized Pt	2109–2113	$\nu(CO)$	
Cyanide (–CN)	2135–2150	$\nu(C{\equiv}N)$	[23,29,30]
Isocyanates (–NCO) on support	2230–2250	$\nu(N{=}C{=}O)$	[23,30–34]
Isocyanates (–NCO) on metal	2173–2192	$\nu(N{=}C{=}O)$	[25,55,59–62]

assigned to bridging nitrite or chelating nitro species [22 and references therein]. For Pt/Al_2O_3 at 200 °C, we observed the same bands for NO + O_2 adsorption, whereas CO (or C_3H_6) + O_2 adsorption resulted in barely detectable features in the 1650–1150 cm^{-1} region. These observations further support the above assignments to nitroxy species.

The temperature dependence of the DRIFT spectra is revealing. It is apparent from Fig. 2 that at 300 °C significant attenuation of the bands at 1230 and 1316 cm^{-1} occurred, reflecting the high reactivity of the nitro/nitrite species. At the same time, weak bands appeared at 2148, 2232 and 2250 cm^{-1} attributed to cyanide [23,29,30], and isocyanate (2232 and 2250 cm^{-1}) on two different types of Al^{3+} sites, respectively [23,30–34]. Above 350 °C the intensity of carbonyl bands (2113 and 2060 cm^{-1}) gradually decreased, whereas new bands at 2995, 2905, 1590, 1550, 1447, 1393 and 1373 cm^{-1} appeared, their intensities progressively increasing with temperature. The features at 1590, 1393 and 1373 cm^{-1} are in a good agreement with spectra obtained for formic acid adsorbed on Al_2O_3 [35] and thus are assigned to $\nu_{as}(COO^-)$, $\delta(CH)$ and $\nu_s(COO^-)$ respectively, of formate ions on Al_2O_3 [23,24,32–36]. Equally, the bands at 1550 and 1447 cm^{-1} can be attributed to $\nu_{as}(COO^-)$ and $\nu_s(COO^-)$ stretches, respectively, of adsorbed acetate on Al_2O_3 [23,24,32–36]. The onset of these bands at 350 °C indicates that reactions involving C_3H_6 became significant at this temperature. The increased intensity of the carboxylate bands with temperature is consistent with the appearance of weak bands in the C–H region (2900–3000 cm^{-1}) at 2905 and 2995 cm^{-1}, which are due to adsorbed hydrocarbon fragments from propene or from alkyl groups associated with carboxylate species [23,24,33].

Fig. 4 shows corresponding IR spectra acquired under identical conditions with the Pt/Al–(Ce–La) catalyst, promoted by modifying the Al_2O_3 support with CeO_2 and La_2O_3 (Table 1). In the low frequency region (1650–1150 cm^{-1}), where nitroxy species (1316 and 1230 cm^{-1}), formates (1591, 1393, and 1373 cm^{-1}) and acetates (1551 and 1447 cm^{-1}) appear, there are no significant differences between these spectra and those presented in Fig. 2. The only notable difference between the spectra in Fig. 4 (Pt/Al–Ce–La) and Fig. 2 (Pt/Al) is the appearance of carboxylate species at a lower temperature, i.e., ~300 °C for the promoted support rather than 350 °C. This may indicate that CeO_2 and La_2O_3 incorporation promotes propene activation *via* the formation of carboxylates, which are thought to be reaction intermediates in propene oxidation [24,32].

In the high frequency region (2300–1800 cm^{-1}) the main difference between the Pt/Al–(Ce–La) (Fig. 4) and Pt/Al (Fig. 2) catalysts is in the intensity of the bands at 2060 and 2109 cm^{-1}, assigned to CO species adsorbed on reduced (Pt^0) and positively charged ($Pt^{\delta+}$) sites, respectively. Specifically, the CeO_2–La_2O_3 modified Pt/γ-Al_2O_3 sample shows (Fig. 4) significant CO populations on both reduced (2060 cm^{-1}) and oxidized (2109 cm^{-1}) Pt sites, whereas for the un-promoted Pt/Al sample (Fig. 2) CO is mainly associated with $Pt^{\delta+}$ (2109 cm^{-1}). This difference implies that incorporation of CeO_2 and La_2O_3 into the γ-Al_2O_3 support significantly modifies the oxidation state of Pt. As Pt^0 sites are considered to be more active [27,37] in TWC catalytic chemistry, this finding provides a basis for rationalizing not only our own results (Fig. 1) but also those obtained by others [28,38–40]. Thus Kotsifa et al. [39] showed that Pt crystallites supported on Al_2O_3 are partially oxidized following interaction with NO, whereas ZrO_2 and CeO_2 maintained the Pt in a more reduced state. In this

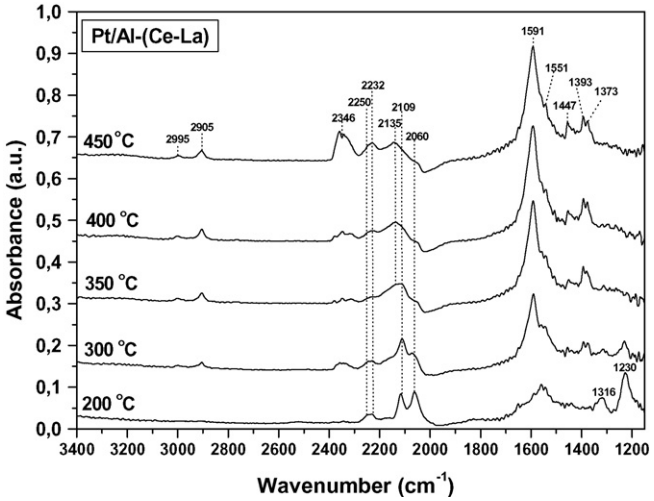

Fig. 4. DRIFT spectra of Pt/Al–(Ce–La) catalyst at various temperatures under simulated exhaust conditions. FT-IR chamber feed: 0.1% NO + 0.1067% C_3H_6 + 0.7% CO + 0.78% O_2; total flow 80 cm^3/min. Each spectrum has been taken 30 min after the desired temperature reached.

connection, Riguetto et al. [28] investigated CO adsorption on Pt/Al_2O_3–CeO_2 and Pt/Al_2O_3 catalysts and suggested that the morphology and electronic state of Pt particles is strongly influenced by the presence of CeO_2. TPR, EPR and FTIR studies by Martínez-Arias et al. [40] indicated that the presence of CeO_2 in Pt/Al_2O_3 catalysts promotes Pt reduction. Finally, we note that single crystal studies of the Pt/ceria system provide clear evidence that submonolayer ceria coverage strongly promote CO oxidation [41].

Our results do not permit discrimination between (a) modification occurring at Pt sites in close contact with Al_2O_3 or (b) only at Pt sites interfaced with the rare earth oxide component. Literature reports on NO or CO chemisorption on Pt catalysts supported on bare Al_2O_3, CeO_2 or mixed Al_2O_3–CeO_2 carriers [38–40] indicate that modifications in oxidation state of Pt are principally related with Pt–rare earth oxide interactions, including the following possibilities:

(i) SMSI between Pt and CeO_2;
(ii) changes in morphology of Pt crystallites dispersed on CeO_2-modified Al_2O_3;
(iii) CeO_2 may provide highly reactive oxygen species at the metal–support interface;
(iv) interaction between Pt and CeO_2 enhances Pt reducibility, thus providing sites for CO activation.

All these possibilities seem plausible but we are unable to distinguish between them due to lack of relevant information because the presence of CeO_2 in the support of some samples vitiates metal dispersion measurements by conventional H_2 or CO chemisorption methods [42]. Our earlier work on Pt/Al and Pt(Na)/Al catalysts prepared by the same procedure showed dispersions that varied by 20–30%. Such variability in dispersion is definitely insufficient to explain the very large changes in performance induced by Na addition [e.g., 9,13]. A similar situation and arguments are expected to hold for the present results. Moreover, Kotsifa et al. [39] showed that for Pt/Al_2O_3, Pt/ZrO_2 and Pt/CeO_2 catalysts with similar Pt dispersions, significant differences occurred in the oxidation state of Pt, an effect that was attributed to interaction of ZrO_2 and CeO_2 oxides with Pt.

Fig. 5 depicts spectra acquired under corresponding conditions for the *doubly-promoted catalyst* Pt(Na)/Al–(Ce–La) for which both support-mediated promotion and promotion of the Pt component directly by Na are expected. Significant differences are apparent between the behaviour of this catalyst (Fig. 5) and that of both the Pt/Al (Fig. 2) and the Pt/Al–(Ce–La) (Fig. 4) catalysts. These differences which related to the bands in both the low (1650–1100 cm^{-1}) and high (2300–1800 cm^{-1}) frequency regions are summarized below:

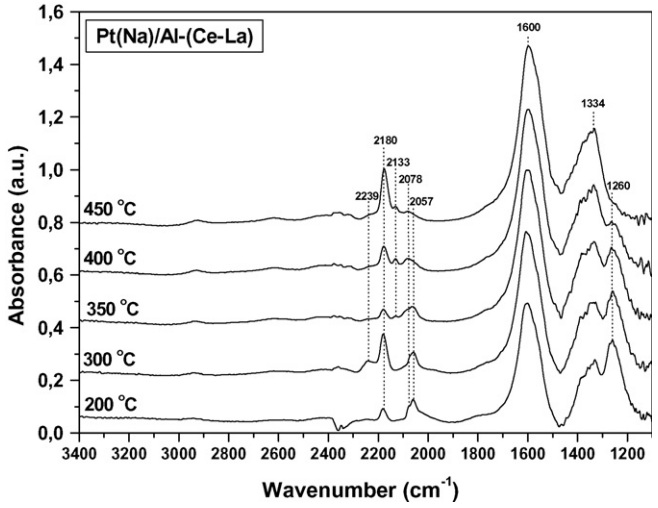

Fig. 5. DRIFT spectra of Pt(Na)/Al–(Ce–La) catalyst at various temperatures under simulated exhaust conditions. FT-IR chamber feed: 0.1% NO + 0.1067% C_3H_6 + 0.7% CO + 0.78% O_2; total flow 80 cm^3/min. Each spectrum has been taken 30 min after the desired temperature reached.

(i) For the doubly promoted catalyst (Fig. 5), interaction with simulated automotive exhaust gas (NO + O_2 + CO + C_3H_6) at 200 °C leads to the formation of significantly greater amounts of nitroxy species compared to the Na-free, Pt/Al (Fig. 2) and Pt/Al–(Ce–La) (Fig. 4) catalysts under identical conditions, as indicated by the appearance of the intense band at 1260 cm^{-1}, assigned to nitrite ion [22]. The broad bands centred at 1600 and 1334 cm^{-1} (Fig. 5) are consistent with those observed during interaction of CO + O_2 with Pt(Na)/Al–(Ce–La) catalyst (data not shown here); it is therefore reasonable to assign these bands to carbonates [43–45], although, carboxylates and/or nitrates are also expected to contribute in these frequency region (Fig. 5). With increasing temperature the nitrite band at 1260 cm^{-1} is progressively attenuated, whilst those at 1600 and 1334 cm^{-1} increased in intensity, maximizing at 450 °C, at which point the nitrite band had almost disappeared (Fig. 5), reflecting the high reactivity of nitroxy species under reaction conditions.
(ii) The surface of Pt(Na)/Al–(Ce–La) catalyst appears to be predominantly covered by nitroxy species and carbonates (Fig. 5) as opposed to the carboxylates and hydrocarbon fragments that are characteristic of the Pt/Al (Fig. 2) and Pt/Al–(Ce–La) (Fig. 4) catalysts. Given the relatively low activity of Na-free catalysts under our conditions (Fig. 1) this observation suggests that carboxylates are spectator species whereas nitroxy species are reaction intermediates.
(iii) In the 2300–1800 cm^{-1} region, the Pt(Na)/Al–(Ce–La) catalyst (Fig. 5) is characterized by the absence of carbonyl species on $Pt^{\delta+}$ sites (2109 cm^{-1}) in contrast to the Pt/Al–(Ce–La) (Fig. 4) and especially the Pt/Al (Fig. 2) catalyst where these species are present.
(iv) The Pt(Na)/Al–(Ce–La) catalyst (Fig. 5) exhibits a very characteristic band at 2180 cm^{-1} which is absent from the Pt/Al (Fig. 2) and Pt/Al–(Ce–La) (Fig. 4) spectra obtained under the same conditions. This is tentatively attributed to NCO species adsorbed on Pt sites (see below).

Points (iii) and (iv) are exemplified more clearly in Fig. 6 which depicts expanded scale spectra for the 2300–1800 cm^{-1} region for all samples at 200 °C. The absence of bands in this region for all the Pt-free materials is very evident, namely: Al_2O_3, Na/Al_2O_3, Al_2O_3–CeO_2–La_2O_3, Na/Al_2O_3–CeO_2–La_2O_3 (spectra A, B, C and D, respectively). The Pt-containing samples show several bands in the 2300–1800 region; these are strongly dependent on the support material. Specifically, spectrum E (un-promoted Pt/Al catalyst) is dominated by a strong band at 2115 cm^{-1}, which is assigned to CO species on $Pt^{\delta+}$, and a very weak band at 2060 cm^{-1} attributed to CO species adsorbed on reduced Pt sites (Pt^0). Spectrum F (Pt/Al–(Ce–La) catalyst) shows bands at 2060 and 2115 cm^{-1} whose intensities are, respectively, higher and lower than in spectrum E, confirming that rare earth oxides significantly alter the oxidation state of Pt.

Interestingly, addition of Na to Pt/Al or Pt/Al–Ce–La catalysts to produce Pt(Na)/Al and Pt(Na)/Al–Ce–La samples (spectra G and H respectively in Fig. 6) did not resulting a band at 2115 cm^{-1}. Instead, two partially resolved bands at 2078 and 2060 cm^{-1} attributed to CO on reduced Pt appeared accompanied by an intense band at 2180 cm^{-1}, assigned to NCO species. The low

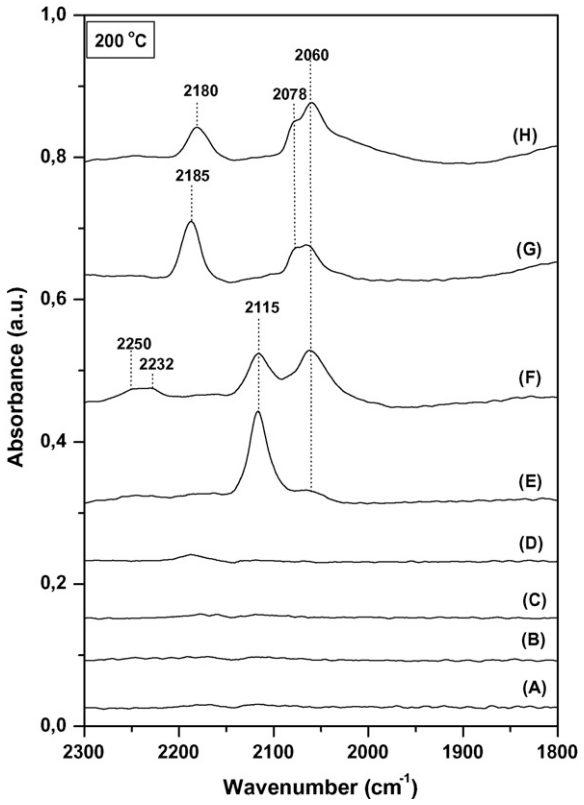

Fig. 6. DRIFT spectra of Al_2O_3 (A), Na/Al (B), Al–(Ce–La) (C), Na/Al–(Ce–La) (D), Pt/Al (E), Pt/Al–(Ce–La) (F), Pt(Na)/Al (G) and Pt(Na)/Al–(Ce–La) (H) in the 2300–1800 cm^{-1} region at 200 °C. FT-IR chamber feed: 0.1% NO + 0.1067% C_3H_6 + 0.7% CO + 0.78% O_2; total flow 80 cm^3/min. Each spectrum has been taken 30 min after the imposed reaction conditions.

frequency band at 2060 cm^{-1} may be associated with adsorption at step sites and the higher frequency band at 2078 cm^{-1} with adsorption on terraces sites [46,47]. Note also that bands at 2060, 2078 and 2180 cm^{-1} only appeared with samples that contained *both* Pt and Na (i.e. Pt(Na)/Al and Pt(Na)/Al–(Ce–La)). This is consistent with alkali-induced charge transfer [21,48], from the Pt Fermi level to the π^* antibonding orbital of CO and concomitant strengthening of the Pt–C bond resulting in Pt^0–CO entities characterized by lower C–O frequencies (2080–2060 cm^{-1}) as opposed to $Pt^{\delta+}$–CO species (2110 cm^{-1}) as indeed observed (Fig. 6).

3.3. Transient DRIFT spectra response of the catalysts under switching from oxidizing to reducing conditions

To elucidate the role of the nitroxy speces that formed in significant amounts only in the case of Na-promoted catalysts, we examined their reactivity towards reducing agents by following the transient response of IR spectra in the temperature interval 200–450 °C for both Na-free and Na-containing catalysts.

Fig. 7 shows spectra obtained with the doubly promoted Pt(Na)/Al–(Ce–La) catalyst after treatment in NO + O_2 flow at 200 °C for 60 min, followed by switching to C_3H_6 + CO flow and temperature increase up to 450 °C. It is clear that the NO + O_2 treatment results in formation of significant amounts of nitroxy species, e.g. the intense band at 1260 cm^{-1}, previously assigned to nitrite (Table 3). Switching to C_3H_6 + CO flow resulted in significant spectral changes. Specifically, the intensity of the 1260 cm^{-1} band decreased progressively with increasing temperature (Fig. 7), reflecting the high reactivity of these species towards hydrocarbon

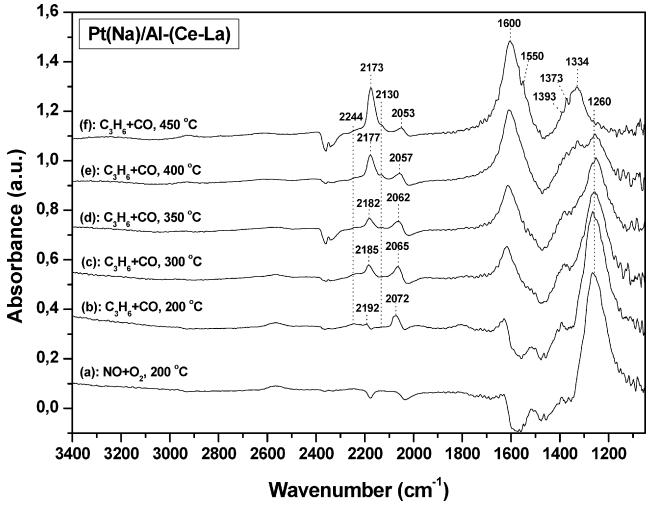

Fig. 7. DRIFT spectra of Pt(Na)/Al–(Ce–La) catalyst, after exposure to 0.1% NO + 0.78% O_2 at 200 °C for 60 min (a) and subsequent switch to 0.1067% C_3H_6 + 0.7% CO at 200 °C (b), 300 °C (c), 350 °C (d), 400 °C (e) and 450 °C (f). Each spectrum has been taken 30 min after the desired temperature reached.

and CO. At the same time, bands appeared at 2244 cm^{-1} (NCO adsorbed on support), 2192 cm^{-1} (NCO on Pt), 2130 cm^{-1} (CN), 2072 cm^{-1} (CO on Pt^0) and also in the 1600–1200 cm^{-1} region (carbonates and carboxylates), the intensities of which increased with temperature. At 450 °C, the 1260 cm^{-1} band had almost disappeared while at the same time the NCO and carboxylate bands attained their maximum intensity.

The progressive shift of the CO band from 2072 cm^{-1} at 200 °C to 2052 cm^{-1} at 450 °C may result from one or more of the following: (i) decreased dipole–dipole coupling between CO chemisorbed molecules with decreasing coverage [25,28,49], (ii) progressive reduction of Pt sites by electron donating adsorbates (e.g. C_3H_6) with increasing temperature [23,49]; this would act to decrease the C–O bond order, thus lowering ν_{CO}.

Fig. 8 shows corresponding spectra for the Na-free Pt/Al which showed the lowest activity under simulated exhaust conditions (Fig. 1). In contrast to the Na-containing catalyst Pt(Na)/Al–(Ce–La) (Fig. 7), in this case interaction with NO + O_2 leads to very limited formation of nitro/nitrite (1316 and 1230 cm^{-1}) and nitrite/nitrate

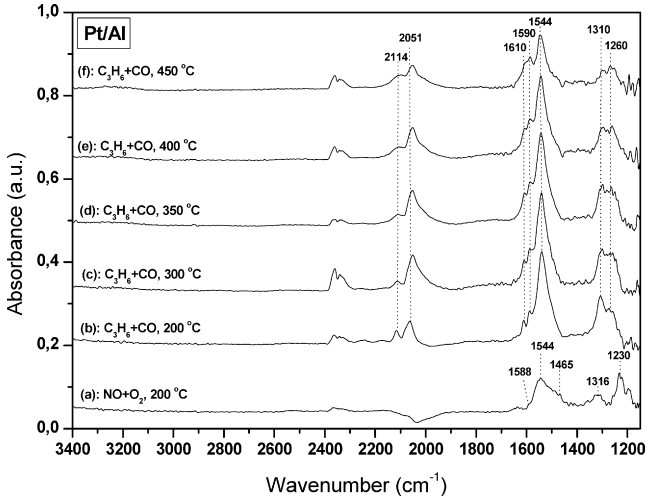

Fig. 8. DRIFT spectra of Pt/Al catalyst, after exposure to 0.1% NO + 0.78% O_2 at 200 °C for 60 min (a) and subsequent switch to 0.1067% C_3H_6 + 0.7% CO at 200 °C (b), 300 °C (c), 350 °C (d), 400 °C (e) and 450 °C (f). Each spectrum has been taken 30 min after the desired temperature reached.

species (1600–1450 cm^{-1}). Switching to C_3H_6 + CO flow resulted only in formation of adsorbed CO (2114 and 2051 cm^{-1}), no NCO bands being observed over the entire temperature range (Fig. 8), in marked contrast to the behaviour of the Na-dosed Pt(Na)/Al–(Ce–La) catalyst (Fig. 7).

In summary, Figs. 7 and 8 show (i) nitroxy species are formed in significant amounts *only* on Na-promoted catalysts and these are very active towards reducing agents [50]; (ii) the NCO band appears only for the Na-promoted samples, consistent with the results obtained under steady state reaction conditions (Fig. 5).

It is generally accepted [51–54] that formation of NCO is preceded by NO dissociation followed by interaction of N(ads) with CO(ads) (or CO(g)) on active metal centers. Accordingly, it has been argued [53,54] that the intensity of the NCO band may be used as an indication of the extent of NO dissociation on active metal sites.

In the light of these literature results and our observation that the ~2180 cm^{-1} band only ever appears with *Na-modified Pt-containing* catalysts (Figs. 5–7) which favour NO dissociation [22], we assign this band to Pt-NCO. It seems clear that the simultaneous presence of both Pt and Na is a necessary and sufficient condition for its formation. This does not preclude the possibility of subsequent NCO migration from Pt sites to other adsorption sites (e.g. Al and Na) where they give rise to bands in the expanded frequency region ~2270–2160 cm^{-1} [58]. This seems a reasonable conclusion, given that 2250–2160 cm^{-1} species (Fig. 6) were only ever detected when NO and CO (or C_3H_6) were *both* present in the reaction gas. Moreover, in earlier studies of NCO formation on platinum single crystal or thin film surfaces [60,62] the band at ~2180 cm^{-1} was assigned to Pt–NCO.

A noteworthy feature is the temperature dependence of the 2192 and 2072 cm^{-1} bands (Fig. 7, 200 °C). As the temperature was increased stepwise from 200 to 450 °C, *both* bands underwent a progressive red shift of 7 cm^{-1}/100 °C. Given that the band initially at 2072 cm^{-1} may be confidently assigned to Pt–CO species, the correlated behaviour of the band initially at 2192 cm^{-1} strongly suggests that this latter band is due to NCO species, also adsorbed on Pt sites. This observation of a simultaneous red shift for both carbonyl and isocyanate species appears to be unprecedented and supports the proposed assignments.

We conclude by considering our results for adsorbed NCO in the light of earlier reports. We argue that Na promotion electronically enhances dissociative adsorption of NO by charge donation into the π^* orbital [22] thus favouring subsequent formation of NCO at Pt sites. Moreover, Davydov [55] proposed that stabilization of adsorbed NCO species at 2200–2100 cm^{-1} can be due to increased electron density in the NCO antibonding orbitals which is in line with our proposal that NCO stabilization occurs at electron enriched Pt sites which are also the source of NO dissociation. In good agreement with this view, Novák and Solymosi [51] found that pre-adsorbed potassium on Rh/SiO_2 catalysts increased the formation of the Rh–NCO species (at 2180 cm^{-1}) during the NO + CO reaction. Finally, Ukisu et al. [52,56,57] reported that Cs increased the efficiency of Cu/Al_2O_3 catalysts towards NOx reduction, an effect they attributed to enhanced isocyanate formation and its subsequent reaction with NO. Thus a consistent picture for alkali promotion of NOx reduction under TWC conditions emerges. There are two electronically driven effects—enhanced dissociation of NO which leads to greater NCO formation and (ii) and activation of this NCO towards subsequent reaction with NO.

In passing we note that alkali promotion by conventional means has often been compared with alkali promotion via the NEMCA effect, for example Refs. [63,64], and consideration given to the roles of alkali cations and the counter-ions that are necessarily present at the catalyst surface [65]. The implications of this work are that conventional chemical promotion by alkalis and NEMCA promotion by alkalis operate in essentially the same way.

4. Conclusions

(i) With Pt/Al_2O_3 catalysts under TWC conditions, formates and acetates are the principal species present on the support, with carbonyls adsorbed at $Pt^{\delta+}$ sites.
(ii) Incorporation of rare earth oxides (CeO_2 and La_2O_3) into the Al_2O_3 support significantly alters the oxidation state of the platinum to Pt^0, with beneficial effects on the activity and selectivity of the catalyst.
(iii) Na-addition leads to even more effective electronic promotion of the Pt component with extensive carbonyl adsorption at electron-rich (fully reduced) Pt sites. Isocyanates are also formed on the platinum and appear to behave as very active reaction intermediates. Isocyanate formation is consistent with electron enrichment of Pt sites by the electropositive sodium promoter which also causes enhanced NO dissociation at such sites.
(iv) Pt^0–CO and Pt^0–NCO, both induced by sodium, are thought to be responsible for the very high activity and selectivity of the Na-promoted catalysts towards TWCs reactions.

Acknowledgements

The authors acknowledge financial support of this work by the PENED 03ED606 research project, implemented within the framework of the "Reinforcement Programme of Human Research Manpower" (PENED) and co-financed by National and Community Funds (75% from E.U.-European Social Fund and 25% from the Greek Ministry of Development-General Secretariat of Research and Technology).

References

[1] J. Kaspar, P. Fornasiero, N. Hickey, Catal. Today 77 (2003) 419.
[2] H.S. Gandhi, G.W. Graham, R.W. McCabe, J. Catal. 216 (2003) 433.
[3] R.J. Farrauto, R.M. Heck, Catal. Today 51 (1999) 351.
[4] V.I. Pârvulescu, P. Grange, B. Delmon, Catal. Today 46 (1998) 233.
[5] I.V. Yentekakis, G. Moggridge, C.G. Vayenas, R.M. Lambert, J. Catal. 146 (1994) 292.
[6] I.R. Harkness, C. Hardacre, R.M. Lambert, I.V. Yentekakis, C.G. Vayenas, J. Catal. 160 (1996) 19.
[7] N.C. Filkin, M.S. Tikhov, A. Palermo, R.M. Lambert, J. Phys. Chem. A 103 (1999) 2680.
[8] M. Konsolakis, I.V. Yentekakis, A. Palermo, R.M. Lambert, Appl. Catal. B 33 (2001) 293.
[9] M. Konsolakis, N. Macleod, J. Isaac, I.V. Yentekakis, R.M. Lambert, J. Catal. 193 (2000) 330.
[10] N. Macleod, J. Isaac, R.M. Lambert, J. Catal. 198 (2001) 128;
N. Macleod, J. Isaac, R.M. Lambert, Appl. Catal. B 33 (2001) 335.
[11] I.V. Yentekakis, V. Tellou, G. Botzolaki, I.A. Rapakousios, Appl. Catal. B 56 (2005) 229.
[12] I.V. Yentekakis, R. Lambert, M. Tikhov, M. Konsolakis, V. Kiousis, J. Catal. 176 (1998) 82.
[13] I.V. Yentekakis, M. Konsolakis, R.M. Lambert, N. Macleod, L. Nalbandian, Appl. Catal. B 22 (1999) 123.
[14] M. Konsolakis, I.V. Yentekakis, Appl. Catal. B 29 (2001) 103.
[15] M. Konsolakis, I.V. Yentekakis, J. Catal. 198 (2001) 142.
[16] N. Macleod, J. Isaac, R.M. Lambert, J. Catal. 193 (2000) 115.
[17] P. Vernoux, A.-Y. Leinekugel-Le-Cocq, F. Gaillard, J. Catal. 219 (2003) 247.
[18] F. Gonçalves, J.L. Figueiredo, Appl. Catal. B 62 (2006) 181.
[19] B. Mirkelamoglou, G. Karakas, Appl. Catal. A 299 (2006) 84.
[20] F. Dorado, A. de Lucas-Consuegra, P. Vernoux, J.L. Valverde, Appl. Catal. B 73 (2007) 42.
[21] N.D. Lang, S. Holloway, J.K. Norskov, Surf. Sci. 150 (1985) 24.
[22] S. Koukiou, M. Konsolakis, R.M. Lambert, I.V. Yentekakis, Appl. Catal. B 76 (2007) 101.
[23] D.K. Captain, M.D. Amiridis, J. Catal. 184 (1999) 377.
[24] W. Schießer, H. Vinek, A. Jentys, Appl. Catal. B 31 (2001) 263.
[25] J.-L. Freysz, J. Saussey, J.-C. Lavalley, P. Bourges, J. Catal. 197 (2001) 131.

[26] S.-C. Shen, S. Kawi, J. Catal. 213 (2003) 241.
[27] O.S. Alexeev, S.Y. Chin, M.H. Engelhard, L. Ortiz-Soto, M.D. Amiridis, J. Phys. Chem. B 109 (2005) 23430.
[28] B.A. Riguetto, S. Damyanova, G. Gouliev, C.M.P. Marques, L. Petrov, J.M.C. Bueno, J. Phys. Chem. B 108 (2004) 5349.
[29] F.C. Meunier, J.P. Breen, V. Zuzaniuk, M. Olsson, J.R.H. Ross, J. Catal. 187 (1999) 493.
[30] N. Bion, J. Saussey, M. Haneda, M. Daturi, J. Catal. 217 (2003) 47.
[31] T. Venkov, M. Dimitrov, K. Hadjiivanov, J. Mol. Catal. A 243 (2006) 8.
[32] M. Haneda, N. Bion, M. Daturi, J. Saussey, J.-C. Lavalley, D. Duprez, H. Hamada, J. Catal. 206 (2002) 114.
[33] G.R. Bamwenda, A. Ogata, A. Obutchi, J. Oi, K. Mizuno, J. Skrzypek, Appl. Catal. B 6 (1995) 311.
[34] M. Huuhtanen, T. Kolli, T. Maunula, R.L. Keiski, Catal. Today 75 (2002) 379.
[35] K. Shimizu, H. Kawabata, A. Satsuma, T. Hattori, J. Phys. Chem. B 103 (1999) 5240.
[36] Ch. He, K. Köhler, Phys. Chem. Chem. Phys. 8 (2006) 898.
[37] R. Burch, P.J. Millington, Catal. Today 26 (1995) 185.
[38] J. Kašpar, P. Fornasiero, M. Graziani, Catal. Today 50 (1999) 285.
[39] A. Kotsifa, D.I. Kondarides, X.E. Verykios, Appl. Catal. B 72 (2006) 136.
[40] A. Martínez-Arias, J.M. Coronado, R. Cataluña, J.C. Conesa, J. Soria, J. Phys. Chem. B 102 (1998) 4357.
[41] Ch. Hardacre, R.M. Ormerod, R.M. Lambert, J. Phys. Chem. 98 (1994) 10901.
[42] S. Bernal, J.J. Calvino, M.A. Cauqui, J.M. Gatica, C. Larese, J.A. Perez Omil, J.M. Pintado, Catal. Today 50 (1999) 175.
[43] C. Morterra, G. Magnacca, Catal. Today 27 (1996) 497.
[44] K. Shimizu, J. Shibata, H. Yoshida, A. Satsuma, T. Hattori, Appl. Catal. B 30 (2001) 151.
[45] E. Fridell, M. Skoglundh, B. Westerberg, S. Johansson, G. Smedler, J. Catal. 183 (1999) 196.
[46] K. Tanaka, J.M. White, J. Catal. 79 (1983) 81.
[47] O. Pozdnyakova, D. Teschner, A. Wootsch, J. Kröhnert, B. Steinhauer, H. Sauer, L. Toth, F.C. Jentoft, A. Knop-Gericke, Z. Paál, R. Schlögl, J. Catal. 237 (2006) 1.
[48] G. Blyholder, J. Phys. Chem. 68 (1964) 2772.
[49] M. Primet, J. Catal. 88 (1984) 273.
[50] U. Bentrup, M. Richter, R. Fricke, Appl. Catal. B 55 (2005) 213.
[51] É. Novák, F. Solymosi, J. Catal. 125 (1990) 112.
[52] Y. Ukisu, S. Sato, A. Abe, K. Yoshida, Appl. Catal. B 2 (1993) 147.
[53] M. Fernández-Garcia, A. Martínez-Arias, A. Iglesias-Juez, A.B. Hungría, J.A. Anderson, J.C. Conesa, J. Soria, J. Catal. 214 (2003) 220.
[54] A. Iglesias-Juez, A. Martínez-Arias, M. Fernández-Garcia, J. Catal. 221 (2004) 148.
[55] A.A. Davydov, J. Appl. Spectrosc. 54 (1991) 287.
[56] Y. Ukisu, S. Sato, G. Muramatsu, K. Yoshida, Catal. Lett. 16 (1992) 11.
[57] Y. Ukisu, S. Sato, G. Muramatsu, K. Yoshida, Catal. Lett. 11 (1991) 177.
[58] N. Bion, J. Saussey, C. Hedouin, T. Seguelong, M. Daturi, Phys. Chem. Chem. Phys. 3 (2001) 4811.
[59] H.Y. Huang, R.Q. Long, R.T. Yang, Energy Fuels 15 (2001) 205.
[60] J.H. Miners, A.M. Bradshaw, P. Gardner, Phys. Chem. Chem. Phys. 1 (1999) 4909.
[61] F. Solymosi, J. Rasko, Appl. Catal. 10 (1984) 19.
[62] J. Rasko, F. Solymosi, J. Catal. 71 (1981) 219.
[63] I.V. Yentekakis, M. Konsolakis, R.M. Lambert, A. Palermo, M. Tikhov, Solid State Ionics 136/137 (2000) 783.
[64] F.J. Williams, A. Palermo, M.S. Tikhov, R.M. Lambert, J. Phys. Chem. B 105 (2001) 1381.
[65] R.M. Lambert, in: A. Wieckowski, et al. (Eds.), Catalysis and Electrocatalysis at Metal Surfaces, Marcel Decker, New York, 2003 (Chapter 16).